Dynamics of Atmospheres and Oceans 71 (2015) 1–20

Contents lists available at ScienceDirect

Dynamics of Atmospheres and Oceans

journal homepage: www.elsevier.com/locate/dynatmoce

Exceptional Bora outbreak in winter 2012: Validation and analysis of high-resolution atmospheric model simulations in the northern Adriatic area

Silvio Davolio[a,*], Paolo Stocchi[a], Alvise Benetazzo[b], Emanuele Bohm[c], Francesco Riminucci[d,e], Mariangela Ravaioli[d], Xiao-Ming Li[f], Sandro Carniel[b]

[a] Institute of Atmospheric Sciences and Climate, CNR ISAC, Via Gobetti 101, 40129 Bologna, Italy
[b] Institute of Marine Sciences, CNR ISMAR, Arsenale Tesa 104, Castello 2737/F, 30122 Venice, Italy
[c] Institute of Atmospheric Sciences and Climate, CNR ISAC, Via Fosso del Cavaliere 100, 00133 Rome, Italy
[d] Institute of Marine Sciences, CNR ISMAR, Via Gobetti 101, 40129 Bologna, Italy
[e] Proambiente S.c.r.l., c/o CNR ISMAR, Via Gobetti 101, 40129 Bologna, Italy
[f] Institute of Remote Sensing and Digital Earth (RADI), Chinese Academy of Sciences, No.9 DengZhuang Nan Road, Haidian, 100094 Beijing, China

ARTICLE INFO

Article history:
Received 24 November 2014
Received in revised form 8 April 2015
Accepted 5 May 2015
Available online 7 May 2015

Keywords:
Bora
Surface fluxes
NWP model
Validation

ABSTRACT

The Bora wind event occurred in winter 2012 was exceptional in terms of both meteorological effects and impact on the Adriatic Sea circulation. It was associated with intense and persistent winds, very cold temperatures all over the Mediterranean basin and heavy snowfall over the Apennines slopes exposed to north-easterly winds, and it was responsible for triggering dense water formation and driving basin-scale oceanic circulation. The cooling period (29 January–13 February) was characterized by intense air–sea exchanges of momentum and heat, whose accurate simulation is required for a proper description of atmospheric and ocean circulations.

In the present study, results of a number of short-range high-resolution numerical weather prediction (NWP) model simulations for the entire Bora outbreak are discussed. The modeling chain, based on BOLAM and MOLOCH limited area models, has been implemented using initial and boundary conditions provided by different global NWP systems. Model performance has been evaluated in terms of variables of interest for oceanographic applications, such as sea surface temperature (SST), surface heat fluxes, solar radiation and near surface meteorological parameters (air temperature, wind, pressure and humidity). The validation has been undertaken through a comparison against surface data (buoys and oceanographic platforms) available at different locations in the northern Adriatic area, while advanced synthetic aperture radar (ASAR) products have been used to assess modeled wind fields on a larger scale.

Model results indicate a good agreement with the observations concerning meteorological variables, in particular wind, pressure and temperature. However, large differences were found in the SST forecasts, which in turn affect also sea surface flux predictions. The uncertainties in SST forecasts are mainly ascribable to the different initialization fields provided by either the global models or satellite analyses. Thus SST initialization represents a critical issue for an accurate description of surface fluxes at least for this exceptionally severe event.

* Corresponding author. Tel.: +39 0516399620; fax: +39 0516399658.
E-mail address: S.Davolio@isac.cnr.it (S. Davolio).

http://dx.doi.org/10.1016/j.dynatmoce.2015.05.002
0377-0265/

1. Introduction

The northern Adriatic Sea is a shallow and semi enclosed basin, and meteorological conditions may remarkably impact the ocean, being responsible for a large variability in current, temperature and salinity. This is especially true during Bora events, typical in the winter season, when the Adriatic Sea is affected by cold and strong winds blowing from the northeast (Grisogono and Belušić, 2009). Bora events are characterized by intense air–sea heat and momentum exchanges (Stravisi and Crisciani, 1986; Mihanović et al., 2013; Stravisi and Crisciani, 1986; Raicich et al., 2013), thus producing strong effects on the thermohaline properties and circulation of the entire Adriatic Sea. In particular, shelf dense-water formation (DWF) processes (Vilibić and Supić, 2005; Mihanović et al., 2013; Benetazzo et al., 2014) are triggered on the broad, shallow shelf in the northernmost region of the Adriatic basin by the cold and severe Bora winds, which bring cold and dry air from the northeastern Europe, down the Dinaric Alps. The resulting intense evaporation and cooling of the shelf waters produce the North Adriatic Dense Water (NAdDW) (Artegiani et al., 1997; Vilibić and Supić, 2005), which then sinks and flows as a dense bottom current along the western Adriatic continental shelf. NAdDW descends all the way to the southern part of the basin, finally affecting the whole deep eastern Mediterranean circulation (Robinson et al., 2003). In particular, during the exceptional cold air outbreak of winter 2012, characterized by prolonged and severe Bora episodes, shelf and coastal DWF occurred not only at the classical sites, but also at a number of eastern Adriatic coastal channels and bays (Mihanović et al., 2013), and the winter 1929 record of density (about 1030.3 kg/m^3; Vatova, 1934) was broken (Raicich et al., 2013Raicich et al., 2013).

Given the impact in terms of meteorological and ocean dynamics, different modeling and observational studies on the Adriatic area have emerged in the past, focused on the analysis of structure and evolution of specific Bora cases and the induced ocean response. Among the modeling studies, Enger and Grisogono (1998) found high correlation between the sea surface temperature (SST) and the Bora offshore propagation length in a series of numerical experiments using a 2D model. Changing the SST turned out to alter the coastal atmospheric boundary layer buoyancy frequency and, as a consequence, the dynamical development of the wind. Later, Cesini et al. (2004) and Kraljević and Grisogono (2006), performing independent 3D modeling analyses of a Bora event in the northern Adriatic, confirmed the impact of SST on Bora characteristics. In particular, Cesini et al. (2004) used also satellite data for a comparison with model simulations and showed that in turn, the Bora flow was able to produce an SST decrease in the affected areas, reaching 7–8 K, locally, in 48 h.

More recently, coupled air–sea models have been applied to the study of Bora events. Pullen et al. (2006, 2007),) produced a thorough analysis of air–sea interactions and found that heat flux and wind stress were remarkably attenuated in the two-way coupled runs compared with one-way coupled simulations, in better agreement with available observations. In particular, two-way coupling provided a more realistic SST field characterized by small-scale cold pattern in the northern Adriatic and along the Italian coast, thus stressing the importance of a correct and detailed SST definition for representing air–sea exchange processes associated with Bora.

On the other hand, among the monitoring studies, Dorman et al. (2007) exploited the data provided by an oceanographic field experiment in the northern Adriatic to characterize heat fluxes associated with a Bora event in winter 2003. More recently, several studies focused on the exceptional Bora episode of January and February 2012. Mihanović et al. (2013) analyzed the associated exceptional DWF, showing its impact on the whole Adriatic basin and identifying important preconditioning factors, such as low precipitation and river discharge. Raicich et al. (2013)Raicich et al. (2013) performed a detailed analysis in terms of overall air–sea interaction and its effect on the seawater in the Gulf of Trieste, showing the exceptional characteristics of the event compared with past episodes.

As pointed out by Dorman et al. (2007) and Pullen et al. (2006, 2007),) turbulent surface (latent and sensible) heat fluxes and SST variations are the two most important parameters that characterize intense air–sea interactions typical of Bora events. Therefore, their accurate simulation is critical in order to properly describe and understand these atmospheric and ocean circulation processes. Numerical weather prediction (NWP) models, applied to short-range forecasts, usually keep SST fixed at its initial value or allow just slow changes according to surface fluxes. This SST representation is generally unrealistic even for short-range forecasts especially in small and shallow basin like the Adriatic Sea during particular meteorological events such as Bora (Cesini et al., 2004).

This framework motivated the present study aimed at investigating the exceptional Bora episode occurred in winter 2012, when winds blew for more than 10 days, the longest duration since 1979 (Benetazzo et al., 2014). High-resolution NWP models (namely BOLAM and MOLOCH, see Section 2) have been used, driven by two different sets of initial and boundary conditions provided by two global NWP systems, namely GFS-NCEP (Global Forecasting System of the US National Center for Environment Prediction) and IFS-ECMWF (Integrated Forecasting System of the European Centre for Medium-range Weather Forecasts). Additional sensitivity experiments have been carried out performing simulations driven by the same global models, but using a different initial SST field provided by near-real time satellite analyses. Thus, in the present study, the sensitivity of Bora simulations to different driving global datasets has been investigated, focusing in particular on the initialization of the SST field that strongly modulates Bora effects at the surface. In order to attain this aim, a number of short-range atmospheric simulations have been performed to cover the entire period (25 January–15 February 2012) and model performances have been evaluated in terms of variables of interest for oceanographic applications. In addition to meteorological variables, surface fluxes, solar radiation and SST fields have been analyzed. The validation has been undertaken trough a comparison with available sea surface and sub-surface data (from buoys and off-shore oceanographic platforms) that allows to suitably monitor the northern Adriatic area and in particular the area characterized by Bora wind jets. Moreover, synthetic aperture radar (SAR) products have been used to assess simulated wind fields on a larger scale.

These products have already proved very useful (Alpers et al., 2009) in providing information about the detailed spatial structure of the Bora wind and as a reference for model simulations (Signell et al., 2010).

This model evaluation represents a useful assessment and a required preliminary step toward a full coupling between atmospheric and ocean models foreseen in the framework of the Italian flagship project RITMARE (http://www.ritmare.it). It is indeed necessary to assess to what extent the NWP system (BOLAM–MOLOCH) is able to properly capture the low level cold air intrusion, modulated by the narrow orographic gaps, and the evolution of the heat fluxes intensity.

The NWP models and the observational data employed for the validation are described in Section 2. The meteorological situation responsible for the severe Bora event and the main effects on the marine circulation are described in Section 3. Comparison between model simulations and observations, including SAR retrievals, are presented in Section 4 and conclusions are drawn in Section 5.

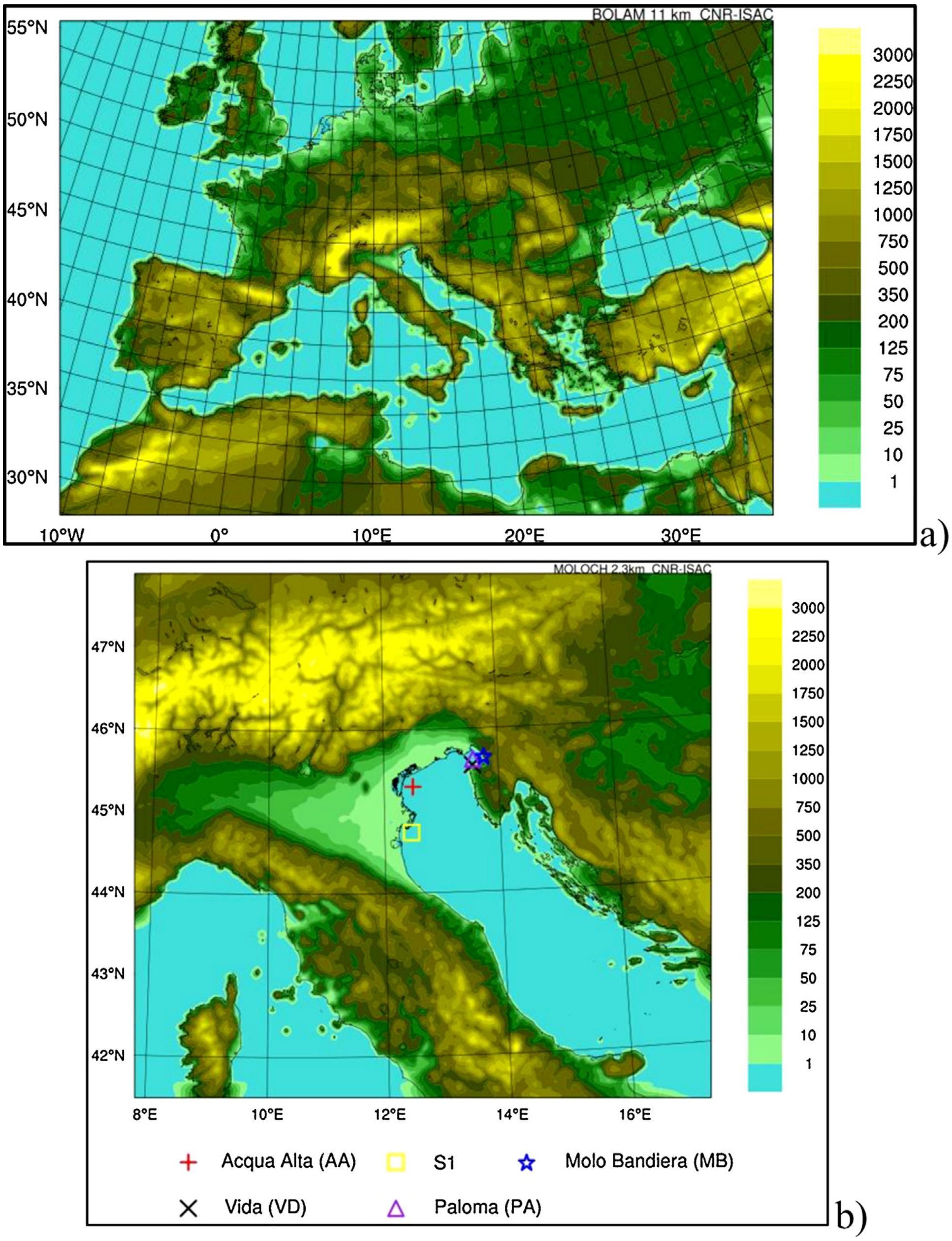

Fig. 1. Integration domain and orography for (a) BOLAM (11 km horizontal resolution) and (b) MOLOCH (2.3 km horizontal resolution) models. Colored dots indicate observations location (buoys and platforms) in the northern Adriatic area employed for the model validation.

2. Data and methodology

2.1. Numerical models

The NWP system employed in the present study is based on BOLAM hydrostatic and MOLOCH non-hydrostatic models. Both models have been developed at the Institute of Atmospheric Sciences and Climate of the Italian National Research Council (CNR-ISAC) and constitute its operational meteorological chain (http://www.isac.cnr.it/dinamica/projects/forecasts). They are being used operationally also at various Italian national agencies and regional meteorological services.

BOLAM and MOLOCH limited area models differ mainly in the dynamical core, in the vertical coordinate discretization, and by the fact that BOLAM includes the Kain–Fritsch – using a modified version based on Kain (2004) – convective parameterization scheme, while in MOLOCH deep convection is explicitly simulated and a simple shallow convection scheme is applied. Atmospheric radiation, atmospheric boundary layer and surface layer parameterizations, soil processes and, to a large extent, microphysical processes are the same in the two models. Considering that the results discussed here are based on MOLOCH simulations, a brief description of the MOLOCH model is provided in the following. For a description of BOLAM see Buzzi et al. (2003),Malguzzi et al. (2006) and Davolio et al. (2006). The BOLAM model (horizontal resolution 11 km) is employed to provide the lateral boundary conditions to the inner grid of the MOLOCH model (horizontal resolution 2.3 km) at 1-h intervals, since the global forecast data are available, at best, every three hours. This current practice has proved reliable and economical in bridging the gap between coarse global model fields (0.5° for the GFS data and about 0.20° for the IFS data) and high-resolution forecasts.

MOLOCH is a non-hydrostatic, fully compressible, convection-permitting model (Malguzzi et al., 2006; Buzzi et al., 2014). It employs a hybrid terrain-following vertical coordinate, depending on air density and relaxing smoothly to horizontal surfaces away from the Earth surface. Time integration is based on an implicit scheme for the vertical propagation of sound waves, while explicit, time-split schemes are implemented for integration of the remaining terms of the equations of motion. Three-dimensional advection is computed using the Eulerian weighted-average flux scheme (Billet and Toro, 1997). The atmospheric radiation is computed with a combined application of the Ritter and Geleyn (1992) scheme and the ECMWF scheme, employing 14 channels for the infrared (IR) and visible bands (Morcrette et al., 2008). The turbulence scheme is based on an E-l, order 1.5 closure theory, where the turbulent kinetic energy equation (including advection) is predicted (Zampieri et al., 2005). Surface turbulent fluxes of momentum, specific humidity and temperature are computed by the classical Monin–Obukhov theory with Businger/Holtslag functions in the unstable/stable case. The mixing length is computed from turbulent kinetic energy (Deardorff, 1980) in the stable atmosphere and from Bougeault and Lacarrere (1989), modified by Zampieri (2004), in the unstable environment. The roughness length is computed as a function of vegetation and of sub-grid orography variance. Over the sea, a Charnock (1955) roughness is introduced, which takes into account the sea roughness as a function of the surface wind speed. The soil model uses seven layers whose depths increase moving downward, and computes surface energy, momentum, water and snow balances, heat and water vertical transfer, vegetation effects at the surface and in the soil. It takes into account the observed geographical distribution of different soil types and soil physical parameters. In particular, the sea temperature (surface and deep sea) is initialized with the SST analysis provided by global model or satellite products. Then, while deep ocean temperature is kept fixed, SST evolves considering a surface layer of about 7 m depth and depending on radiative and latent/sensible heat fluxes. The computation is based on a simple slab ocean model in which the initial analyzed distribution of SST is used as a relaxation reference value (relaxation time of about 2 days), thus allowing a smooth transition toward the deep ocean. The microphysical scheme, recently upgraded, was initially based on the parameterization proposed by Drofa and Malguzzi (2004). The presently applied scheme describes the conversion and interaction of cloud water, cloud ice and hydrometeors (rain, snow, graupel).

In the present study, the NWP system is implemented in order to provide a sequence of short-range atmospheric simulations for the entire period of interest (25 January–15 February). BOLAM (Fig. 1a) is initialized at 00 UTC every day and runs for 36 h, until 12 UTC of the following day. MOLOCH (Fig. 1b) is nested in BOLAM, but its integration is not started at the same instant of the global model analysis (e.g., 00 UTC) in order to avoid numerical problems due to the change in the grid resolution from the global to the 2.3 km grid-spacing, based on pure interpolation. Instead, using a 3-h BOLAM forecast as initial condition allows to have a dynamical downscaling with a suitable ratio between the grids resolutions. MOLOCH run lasts 33 h. Neither data assimilation, nor initialization procedures are applied. The MOLOCH output field for the diagnostic analysis presented in this study is obtained considering the 24-h period 12–12 UTC. Thus, model data are provided continuously for the whole period and the meteorological fields of the very first hours of simulations, possibly affected by spin-up problems, are not considered.

Table 1
Location and instruments height/depth of the monitoring stations in the northern Adriatic basin.

	Molo bandiera (MB)	Paloma (PA)	Vida (VD)	Acqua alta (AA)	S1
Latitude (°N)	45.65	45.62	45.54	45.31	44.74
Longitude (°E)	13.75	13.56	13.55	12.50	12.45
Instruments heights (m)	10	10	5	16	2.5
SST probe depth (m)	2	3	3	1.9	1.8

In addition to the two sets of MOLOCH forecasts driven by the two different global forecasting systems, IFS and GFS (hereafter referred to as IFS-M and GFS-M, respectively) a set of simulations is obtained changing only the initial SST field (SGFS-M). In these experiments, GFS data are used as initial and boundary conditions for BOLAM, except for the initialization of the SST field, which is derived, over the Mediterranean Sea from the operational (near-real time) product of the MyOcean project (http://gosweb.artov.isac.cnr.it) of CNR ISAC at $0.0625 \times 0.0625^{\circ}$ resolution. The SST analyses are obtained starting from IR measurements collected by satellite radiometers and applying the optimal interpolation technique, as described in Buongiorno Nardelli et al. (2013). Only for the small portion of Atlantic Ocean within the BOLAM domain, the SST data is obtained from the OSTIA project of the National Centre for Ocean Forecasting of the UK Met Office, at the resolution of $0.05 \times 0.05^{\circ}$. The BOLAM and MOLOCH initial SST fields are obtained by a suitable merging and resampling the above-mentioned data sources at a common resolution of $1/16^{\circ}$. According to the current operational implementation, the initial SST field is computed by a weighted average between the satellite data and the global model analysis, assigning a weight of 0.8 and 0.2, respectively.

2.2. Meteorological and marine data

Several stations were used to validate the meteorological simulations at representative locations in the northern Adriatic (Fig. 1b) near both the western and the eastern coasts of the basin.

Model performance was evaluated in terms of surface/near-surface variables of interest for oceanographic application, such as 10-m wind speed, 2-m air temperature and relative humidity, surface pressure, turbulent surfaces heat fluxes and solar radiation. Moreover, as representative of the oceanographic side, available SST time series were analyzed. Four stations provided in situ hourly data for air temperature, relative humidity, wind speed and direction, and SST. These stations are (see Fig. 1b and Table 1): Molo Bandiera (MB), situated in an external pier of Trieste harbor; Paloma (Advanced Platform Oceanographic Laboratory Adriatic Sea) mast platform (PM), located in the center of the Gulf of Trieste; Vida buoy (VB), located approximately 2 km off Piran; Acqua Alta oceanographic platform (AA), a fixed oceanographic tower 15 km off the Venice coast. Further measurements used in this work were provided by S1 buoy, located 6 km off the Italian coast, south of the Po river mouth. It is worth noting that at Vida (S1) 10-m wind speed is estimated from the 5-m (2.5-m) data as suggested by Raicich et al. (2013)Raicich et al. (2013).

In addition to meteorological measurements, latent heat (LHF) and sensible heat fluxes (SHF) were provided, computed using different algorithms: at AA and VD, heat fluxes were computed using the coupled ocean atmosphere response experiments (COARE) bulk algorithm (Fairall et al., 2003), while at PM and MB, heat fluxes were estimated via different bulk formulae as described in Raicich et al. (2013)Raicich et al. (2013). A comparison or validation of these formulae is out of the scope of this paper; therefore, although being aware that different bulk formulations may add further uncertainty to fluxes estimation, we prefer to retain the provided original values as presented by the above mentioned studies.

2.3. Synthetic aperture radar data

In the present study, the data acquired by the advanced synthetic aperture radar (ASAR) on-board ENVISAT satellite is used to derive the sea surface wind field at 10-m height for comparison with the model simulations. Fortunately, ASAR

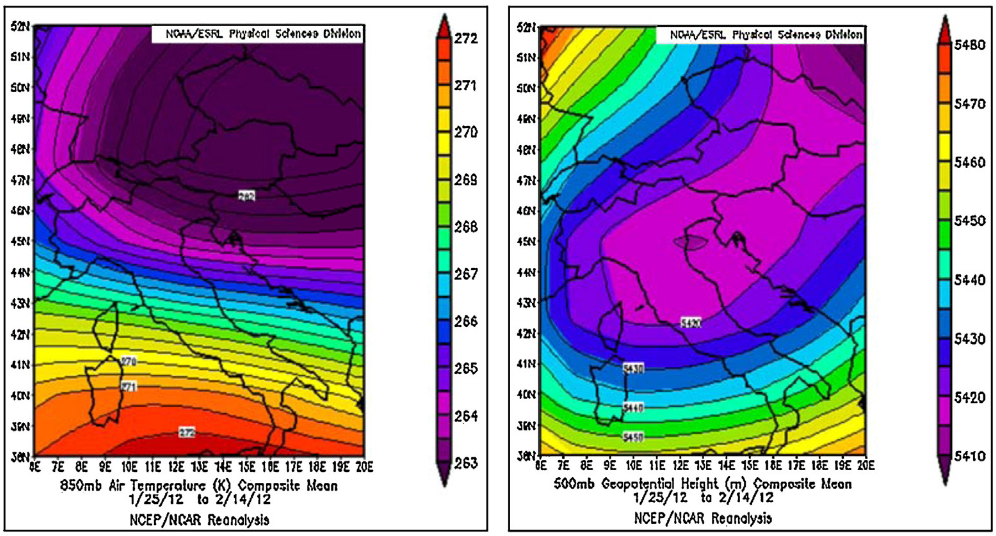

(a) (b)

Fig. 2. (a) 850 hPa temperature (K) and (b) 500 hPa geopotential height (gpm) averaged between 25 January–14 February 2012 (NCEP reanalysis).

acquired a wide swath image with coverage of 400 km × 400 km (thus covering the whole northern Adriatic basin) in vertical–vertical polarization during the exceptional Bora event. The image was acquired on 2 February 2012 at 20:59 UTC.

The sea surface wind field is derived from the ASAR wide swath data using the C-band Geophysical Model Function (GMF) CMOD5 (Hersbach et al., 2007). As the wind streaks are clearly visible in the ASAR image acquired during the Bora event, the sea surface wind direction is derived using the conventional FFT methodology (Lehner et al., 1998). The 180° ambiguity is eliminated based on the fact that the wind blows from northeast during the Bora event. The sea surface wind direction is derived from sub-scenes of 10 km × 10 km, which are further interpolated at high spatial resolution of 500 m × 500 m. Then, the sea surface wind speed is retrieved using the CMOD5.

3. Meteorological and oceanic conditions

By the end of January 2012, the transition from zonal circulation to more meridional flow in the European area was associated with a blocking event characterized by the development of a pressure ridge meridionally elongated over the eastern Atlantic, and by the westward movement of a retrogressive wave from Eurasia toward the Mediterranean basin (Grazzini, 2013). The descent of a cold trough toward central Europe drove very cold air masses of continental origin toward the Mediterranean. As a consequence, until mid February, the Mediterranean basin was characterized by a persistent cyclonic circulation associated with an exceptionally cold anomaly, as shown by the averaged fields of 850 hPa temperature and 500 hPa geopotential height for the period 25 January–14 February 2012 (NCEP Reanalysis, Fig. 2).

Several mesoscale low-pressure systems developed and deepened over the Mediterranean basin during this period. In particular, during 1, 4 and 10 February cyclones formed over the Tyrrhenian Sea and moved quite slowly in the following 36–48 h eastward over the Adriatic Sea. Moreover, an almost stationary cyclonic circulation established over the Ionian Sea between 6 and 7 February. These patterns produced severe wintry conditions characterized by intense snowfalls over northern and central Italy and favoring persistent and strong Bora wind over the Adriatic Sea. In particular, the two heavy precipitation episodes registered in the periods 29 January–02 February and 10–12 February, respectively, were responsible for exceptional snowfall amounts, locally exceeding 3 m along the foothill of the northern Apennines exposed to northeasterly winds. The event was exceptional not only in terms of temperature and precipitation. The persistent pressure gradient across the Balkans, due to the cyclonic condition over the Mediterranean basin, induced long-lasting and strong Bora winds over the northern Adriatic Sea. During the three weeks of windy weather conditions, Bora was strong to severe from east-northeast to northeast, attaining hurricane force locally (Mihanović et al., 2013). Two phases can be recognized during the event, corresponding to the two snowfall periods, separated by an interval of general wind decreasing. The sudden wind speed drop on 12 February clearly marked the end of the episode (Raicich et al., 2013Raicich et al., 2013).

These atmospheric conditions were responsible for intense air–sea energy fluxes over the northern Adriatic Sea (Mihanović et al., 2013). On the one hand, strong and persisting winds caused large momentum transfers from the atmosphere to the ocean (at AA wind stress was modeled as high as 1.5 N/m^2; Benetazzo et al., 2014) that produced a energetic sea state (at AA significant wave height was observed above 1.5 m for about 15 consecutive days), thus forcing the north Adriatic oceanic currents to establish a double-gyre system with surface speed up to 1 m/s (Benetazzo et al., 2014). On the other hand, during the whole Bora event, heat energy loss from the ocean was simulated exceeding 0.5 GJ/m^2 over the northern Adriatic Sea (Mihanović et al., 2013), with peaks up to 1.5 GJ/m^2 on the Bora jets along the eastern shore. Moreover, dry winds caused a considerable evaporation of the water body, which was estimated in the order of 0.2 m over the whole period of the Bora event (Raicich et al., 2013). Combined heat and water fluxes forced the northern Adriatic Sea water temperatures to locally drop to 4 °C (recorded at Paloma station; Raicich et al., 2013) and water densities to generally exceed 1030 kg/m^3 (Raicich et al., 2013; Benetazzo et al., 2014 Benetazzo et al., 2014), a situation therefore favorable for an exceptional production of the NAdDW, a dense water mass that flows toward the southern Adriatic region ventilating deeper water masses and transferring relevant quantities of sediments (Carniel et al., 2012). After the Bora event (approximately on 13 February 2012) the NAdDW occupied most of the Adriatic basin north of Ancona and, driven by Coriolis and gravity forces, started to flow south-eastward (with an average speed of about 0.1 m/s) leaning on the Italian coast in the form of an underflow vein. In the 2–3 months following the Bora event's cessation, dense waters flow produced a considerable renewal of the northern Adriatic waters, since more than 50% of the water volumes were transferred toward the mid- and south-Adriatic by the NAdDW flow. In these regions, heavier waters were partially intercepted by the pits that shape the sea bottom and contributed to replace the older bottom waters that were there resident (Benetazzo et al., 2014). As pointed out by Janeković et al. (2014), these are "fast" processes that took about three weeks from generation in the north to the first arrival of the cold-water signal within the Bari canyon system in the south, about 3 times faster than during average dense water formation episodes according to Vilibić and Orlić (2002).

Thus, the 2012 cooling episode was of major importance for the Adriatic Sea circulation and its effects were traced up to the southern Otranto Strait where the Adriatic connects to the eastern Mediterranean basin. Their relevance goes beyond the regional scale, being the relationships between the variability of the Ionian upper circulation and NAdDW formation at the base of the Bimodal Adriatic-Ionian Oscillation (BiOS, Gačić et al., 2010). With this respect, although we described the processes related to the event per se, it is expected that the recently observed reversals of the upper-layer circulation pattern in the Ionian may play a relevant role in the salt redistribution between the Adriatic and the Levantine basin (Malanotte-Rizzoli et al., 2014), and therefore could be connected, at least on the long climatic term, with the origin of the processes described in this paper.

4. Results

4.1. Comparison against ASAR satellite data

The retrieved sea surface wind from the ASAR wide swath data using the methodology described in Section 2.3 is shown in Fig. 3. Different jets are shown in correspondence with well-known orographic gaps of the Dinaric Alps. The strongest one originates in the Gulf of Trieste and extends westward across the Adriatic, progressively decreasing in intensity, reaching Venice Lagoon. At 2100 UTC, 02 February 2012 (corresponding to the time the image is taken), this jet is very distinct and composed by a single band of intense wind, with instantaneous maximum wind speed close to the eastern Adriatic coast exceeding 25 m/s. South of Istria peninsula, also the jet at Senj appears very intense especially close to the Croatian coast and between the islands. Also this jet is able to affect a large region over the sea, while farther south, the jet at Novalja is more confined to the coastal area. Bora is also quite intense in the area of Zadar. It is worth noting that between each jet band there is a wake area characterized by weak wind, particularly evident west of Istria. As already noted by Dorman et al. (2007), the wind speed decreases more rapidly across the Adriatic away from the northern coast.

MOLOCH simulations are able to capture these features of the wind field. Apparently, its horizontal resolution is high enough to properly describe the critical topographical forcing responsible for the swing of high-speed low-level wind jets and wake areas. Moreover, during this phase of the event, the wind is not deflected in correspondence with the Italian coast, but enters the Po valley from northeast and flows over the Apennines, where heavy precipitation occurs as a consequence of this direct orographic uplift.

A more detailed model evaluation, covering the whole period of severe windy weather, is provided in the following Sections, through a comparison against in situ measurements.

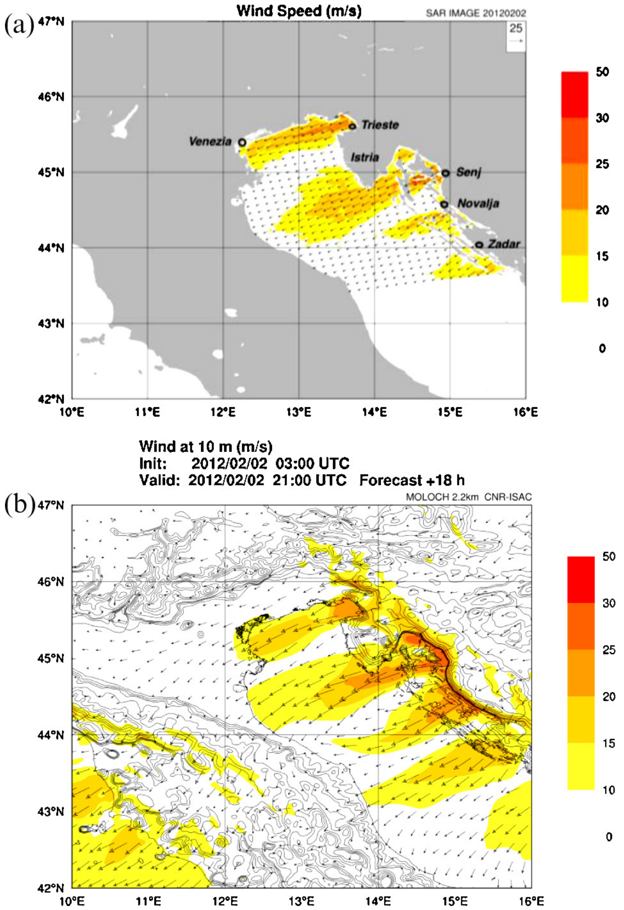

Fig. 3. (a) ASAR retrieved sea surface wind at 10 m height (m/s) using CMOD5 at 2059 UTC, and MOLOCH forecast 10 m wind, at 2100 UTC, 02 February 2012. The main locations cited in the text are reported in (a).

4.2. Comparison with surface meteorological observations

The hourly time series of air temperature, wind speed and direction are shown in Figs. 4 and 5 at different sites in the northern Adriatic. Wind measurements (black dots) clearly mark the onset (28 January) and the rapid conclusion (12 February) of the Bora event. During this period, at least three phases of very intense Bora are shown, namely between 02 and

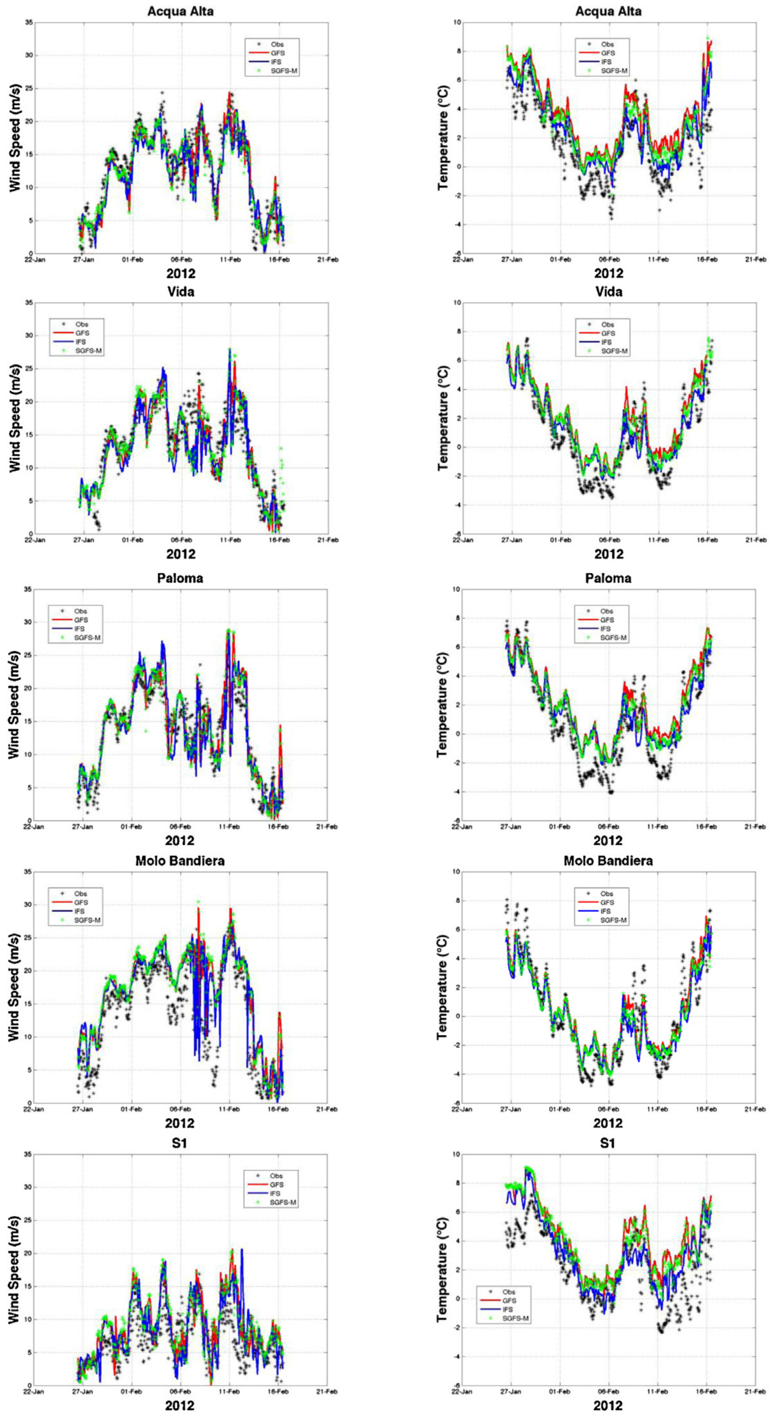

Fig. 4. Time series plot of hourly wind speed (m/s) (left column) and air temperature (°C) (right column) at the observation sites of (from top to bottom) Acqua Alta (AA), Vida (VD), Paloma (PA), Molo Bandiera (MB) and S1 buoy, from 27 January to 16 February 2012. Black stars indicate measurements, colored lines indicate the results of different MOLOCH experiments: IFS-M (blue), GFS-M (red) and SGFS-M (green). (For interpretation of the references to color in this figure legend, the reader is referred to the web version of this article.)

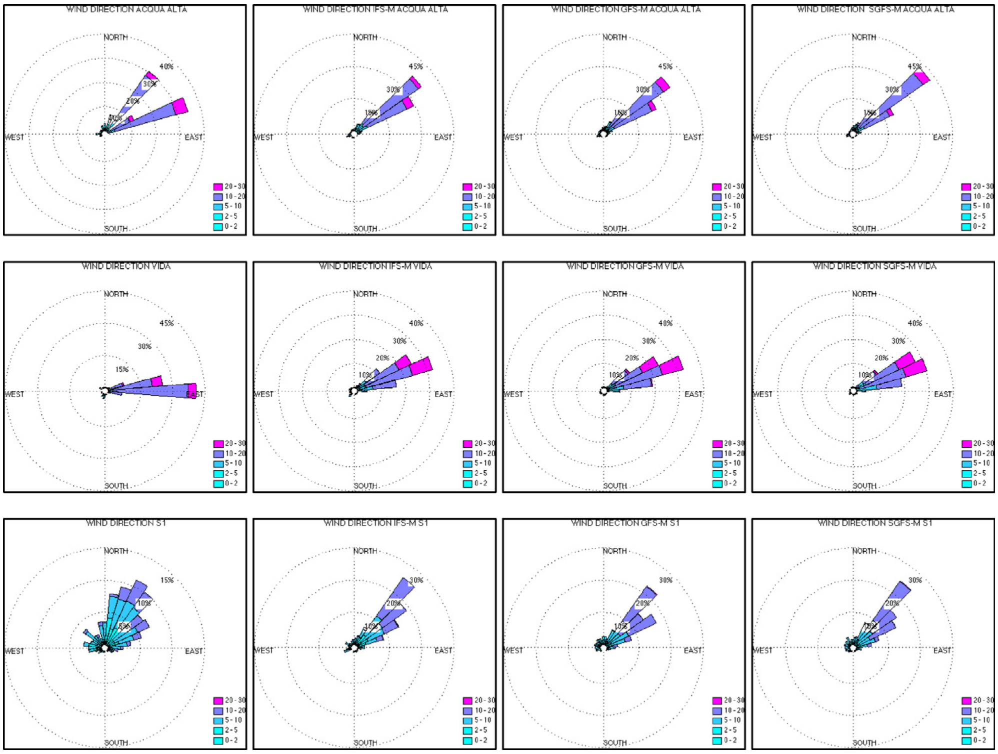

Fig. 5. Wind rose plot of hourly wind direction at the location of Acqua Alta (top), Vida (middle) and S1 buoy (bottom). Observations (left column) and results of different model experiments are shown: IFS-M (second column), GFS-M (third column) and SGFS-M (rightmost column).

04 February, around 7 February and between 10 and 11 February. The temporal evolution is quite similar among the stations, not only in the Gulf of Trieste, but also at AA on the western side of the Adriatic. However, the maximum wind speed is attained at MB (27 m/s on 11 February) and at PA, while slightly lower values are recorded at VD, which possibly remains just outside the main wind jet. At AA the wind speed is very close to PA values, indicating a remarkable propagation of Bora across the entire northern Adriatic Sea. Moving southward along the Italian coast, the wind intensity markedly decreases and at S1 buoy barely exceeds 15 m/s. Moreover, at S1 the evolution of the wind speed is slightly different from the other stations especially during the first phase of the event. This is due to the fact that this buoy is not continuously affected by Bora, as also indicated by wind direction (Fig. 5), which is rather variable, ranging from northwest to east, although maximum intensities are recorded for northeasterly wind. Moreover, at S1 northerly wind is often associated with Bora deflection along the Italian coast, as also noted in Alpers et al. (2009). On the other hand, in the Gulf of Trieste, wind is steadily easterly, as a consequence of the strong topographical forcing producing the Postojna Pass jet, while close to the Venice lagoon a bimodal distribution indicates two preferred wind directions, from northeast and from east-northeast.

The different sets of MOLOCH forecasts provide very similar results concerning near surface (10 m) wind fields, in terms of both intensity and direction. There is a general good agreement with the observed evolution, although the model shows a slight tendency to overestimate the peaks greater than 20 m/s. In particular at S1, MOLOCH overestimates the strong wind periods. However, the uncertainty due to the correction of wind speed from the low height of the instrument (2.5 m) to the level of comparison (10 m) may be relevant. At MB, MOLOCH misses the very low wind phase on 09 February when, at variance with other locations, wind speed dropped below 5 m/s, and in general overestimates the wind speed. Being this station located on the coastline (Trieste harbor), this discrepancy is ascribable to a smaller roughness value associated with the grid point closest to the location of the observation, which results over the sea in the model.

Air temperature presents two separate phases of cooling (Fig. 4), corresponding with two successive cold air outbreaks from continental Europe in the Mediterranean basin. A constant temperature decrease, initiated before the Bora onset, terminated around 03 February, when values below the freezing point was reached at all observation locations. After a steady period lasting three days until 06 February, a temporary warming is observed, preceding a second sharp cooling in correspondence with the last intense Bora period, when the temperature dropped again below 0 °C. MB presents slightly colder values than the other stations, being located close to the coast. The temperature evolution is very similar among the stations, with the only exception being S1 during the last days of observations where it shows larger diurnal oscillations and a more limited increase.

While MOLOCH simulations are able to reproduce closely the temperature fluctuations during the analyzed period, a systematic, although limited overestimation, reaching about 2 °C during the two coldest phases, affects the results. A partial explanation can be provided taking into account that model SST, in all experiments, is generally warmer than observed SST, as will be shown in Section 4.3. However, this cannot completely explain the overestimation since model 2-m air temperatures are very similar among different experiments, while SSTs greatly vary between GFS and IFS driven runs. In well-mixed conditions, as those experienced in the analyzed days due to wind-produced turbulence, the main contribution to the 2-m model temperature comes from the temperature at the first model level, which is approximately 70 m above the ground. It is reasonable to suppose that the planet boundary layer (PBL) parameterization scheme partially attenuates the effect of different SSTs through a vigorous vertical mixing, but overestimates temperature at 2 m.

In order to provide a quantitative assessment of model simulations, correlation, root-mean-square difference (RMSD) and ratio of variance have been computed for wind speed and air temperature. Results are presented (Fig. 6) in Taylor diagrams (Taylor, 2001) for two representative stations located on different sides of the northern Adriatic Sea namely AA and VD. Diagrams confirm the good agreement between simulation and observations as indicated by the high values of correlation and by standard deviation close to observed. Moreover, they also indicate very small differences among different model configurations. Correlation values ranging between 0.8 and 0.9 are obtained also at other observation sites (Table 2), while lower values, although greater than 0.6, are attained only at S1 buoy for wind speed.

The Taylor diagram for temperature (Fig. 6) provides a quantitative confirmation of the analysis of temporal series: a good agreement between model and measurements, with correlation factor up to 0.95 (see Table 2 for the other locations) and negligible differences between different model simulations, as also indicated by the RMSDs and by the mean values.

Model evaluation has been carried out also for near-surface relative humidity (RH) and surface pressure (PS), in order to fully cover the meteorological variable of importance for air–sea interaction. Indeed, RH is related to moisture fluxes from the sea surface, while PS modulates the sea surface elevation thus being a relevant parameter in a region regularly affected by storm surges (e.g., Acqua Alta in Venice lagoon). As shown in Fig. 7, MOLOCH forecasts accurately the surface pressure on

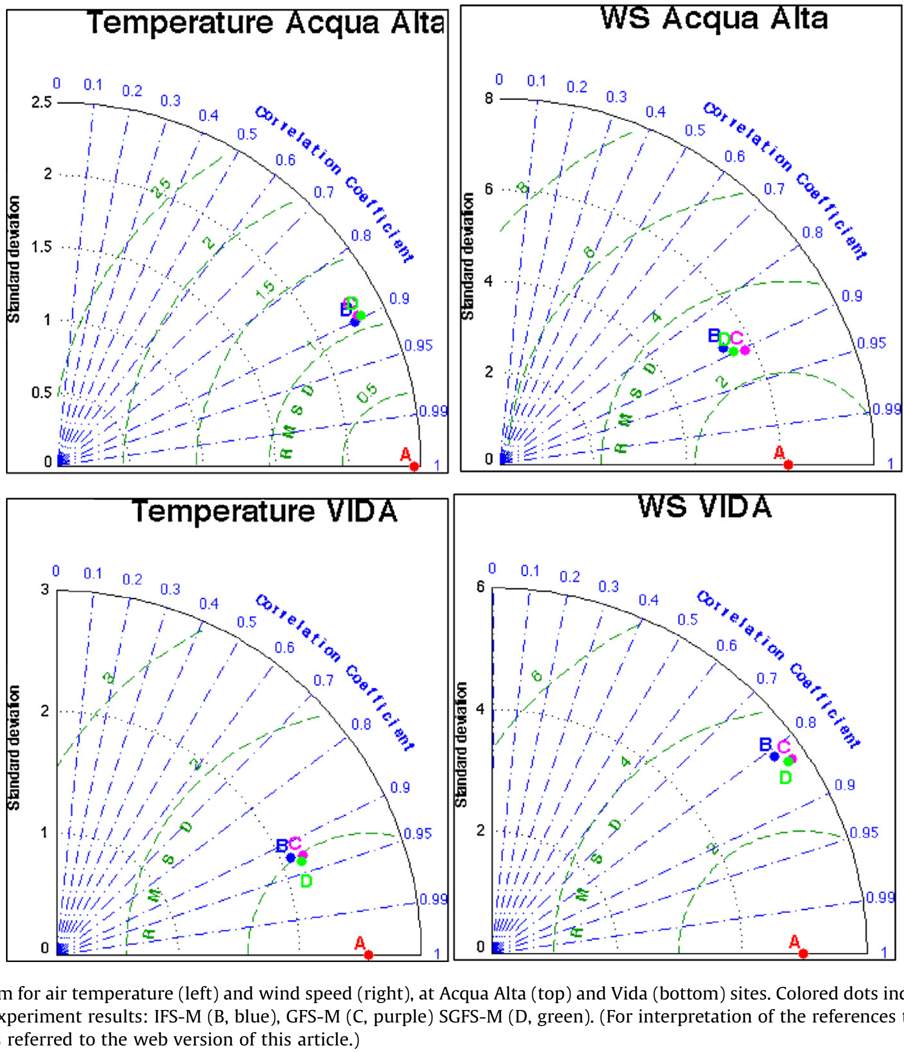

Fig. 6. Taylor diagram for air temperature (left) and wind speed (right), at Acqua Alta (top) and Vida (bottom) sites. Colored dots indicate observation (A, red) and MOLOCH experiment results: IFS-M (B, blue), GFS-M (C, purple) SGFS-M (D, green). (For interpretation of the references to color in this figure legend, the reader is referred to the web version of this article.)

Table 2
Statistical results of the comparison. Mean value, standard deviation, root mean square difference and correlation are reported for all the stations and for the three different sets of model experiments, for temperature, wind speed, SST, surface latent and sensible heat fluxes.

	Temperature				Wind speed				SST				Sensible heat flux				Latent heat flux			
	Mean	STD	RMSD	CORR	Mean	STD	RMSD	CORR	Mean	STD	RMSD	CORR	Mean	STD	RMSD	CORR	Mean	STD	RMSD	CORR
Aqua Alta	274.8	2.5			12.8	6.2			280.8	1.1			−122.0	84.6			−193.4	112.2		
IFS-M	275.7	2.3	1.1	0.9	12.0	5.4	2.9	0.9	280.4	1.0	1.0	0.6	−148.9	96.8	44.4	0.9	−186.9	101.5	51.0	0.9
GFS-M	276.7	2.3	1.1	0.9	12.3	5.8	2.7	0.9	284.3	0.7	1.3	0.1	−234.0	139.3	74.6	0.9	−277.3	142.5	67.9	0.9
SGFS-M	276.2	2.3	1.1	0.9	12.2	5.6	2.7	0.9	283.0	0.8	1.2	0.3	−209.1	124.5	61.0	0.9	−245.4	124.8	52.8	0.9
VIDA	273.6	2.6			12.9	5.0			281.3	1.3			−187.3	106.4			−258.2	112.6		
IFS-M	274.1	2.1	1.0	0.9	13.5	5.6	3.3	0.8	280.8	0.9	1.0	0.7	−229.4	127.9	59.4	0.9	−253.8	117.6	59.1	0.9
GFS-M	274.7	2.2	1.0	0.9	13.8	5.8	3.2	0.8	284.0	0.7	1.4	0.1	−317.3	167.0	86.7	0.9	−345.3	152.0	77.9	0.9
SGFS-M	274.4	2.2	0.9	0.9	13.8	5.7	3.2	0.8	283.3	0.7	1.4	0.1	−301.8	157.8	83.3	0.9	−325.6	142.5	72.9	0.9
PALOMA	274.1	3.1			13.3	6.2			280.3	1.7			−180.9	125.2			−315.1	154.6		
IFS-M	274.7	2.3	1.3	0.9	13.6	6.7	3.2	0.9	280.9	1.0	1.0	0.8	−221.8	140.9	68.7	0.9	−257.8	140.8	73.0	0.9
GFS-M	275.2	2.4	1.1	1.0	13.9	6.7	3.2	0.9	284.0	0.8	1.6	0.3	−310.3	187.0	101.1	0.9	−348.4	176.7	93.6	0.8
SGFS-M	274.9	2.4	1.0	1.0	13.7	6.6	3.1	0.9	283.3	0.8	1.6	0.4	−291.1	175.5	96.5	0.8	−323.3	164.4	89.0	0.8
MOLOBA	273.3	3.2			13.2	7.1			279.9	1.6			−188.7	127.8			−302.3	145.3		
IFS-M	273.1	2.6	1.2	0.9	16.3	6.5	3.9	0.8	280.6	1.1	0.7	0.9	−322.0	171.3	84.6	0.9	−326.5	141.7	75.6	0.9
GFS-M	273.5	2.7	1.2	0.9	16.8	6.5	3.8	0.8	283.6	0.9	1.3	0.6	−435.0	220.3	122.8	0.9	−442.3	179.8	99.1	0.8
SGFS-M	273.3	2.7	1.2	0.9	16.9	6.7	3.8	0.8	282.9	0.9	1.3	0.6	−419.0	214.9	120.8	0.9	−420.9	174.4	95.8	0.8
S1	275.3	2.3			5.6	2.6			279.7	1.5			N.a.	N.a.	N.a.	N.a.	N.a.	N.a.	N.a.	N.a.
IFS-M	276.3	2.5	1.4	0.8	8.3	4.3	3.3	0.6	281.2	1.0	1.6	0.3	N.a.	N.a.	N.a.	N.a.	N.a.	N.a.	N.a.	N.a.
GFS-M	277.3	2.3	1.3	0.8	8.9	4.3	3.2	0.7	284.6	0.5	1.6	−0.1	N.a.	N.a.	N.a.	N.a.	N.a.	N.a.	N.a.	N.a.
SGFS-M	277.1	2.4	1.2	0.9	8.9	4.2	3.1	0.7	284.2	0.7	1.6	−0.007	N.a.	N.a.	N.a.	N.a.	N.a.	N.a.	N.a.	N.a.

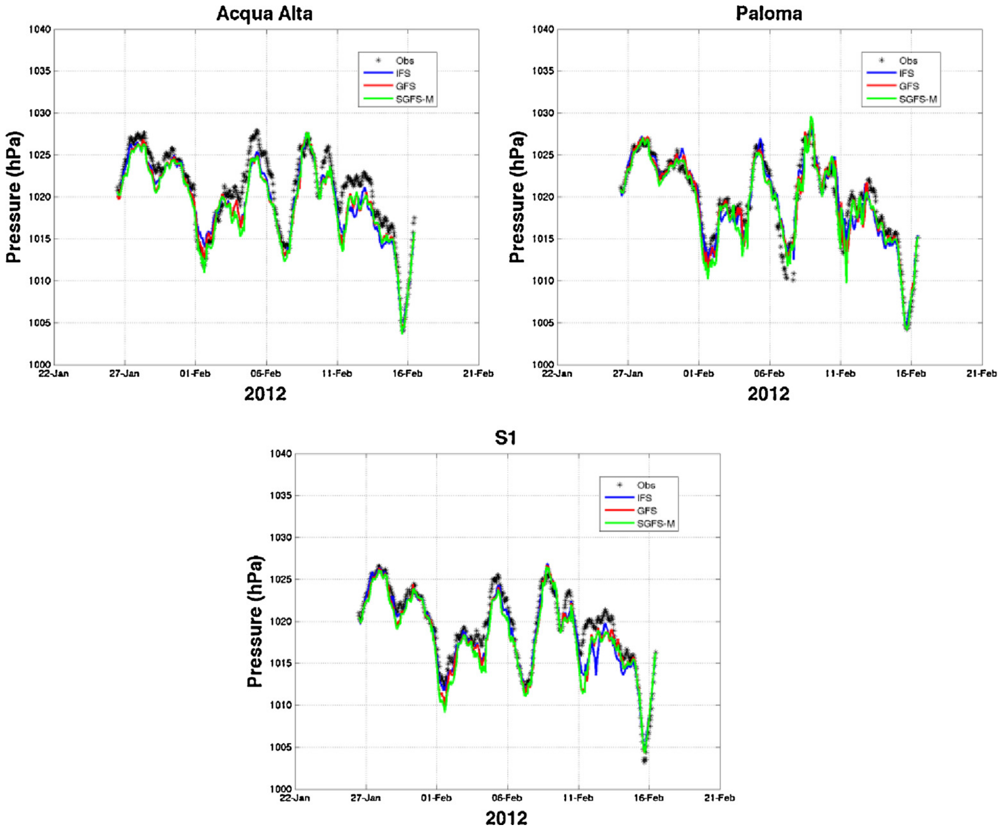

Fig. 7. Time series plot of hourly surface pressure (hPa) at the station Acqua Alta (AA), Paloma (PA), and S1 buoy. Black stars indicate measurements, colored lines indicate the results of different MOLOCH experiments: IFS-M (blue), GFS-M (red) and SGFS-M (green). (For interpretation of the references to color in this figure legend, the reader is referred to the web version of this article.)

both sides of the Adriatic basin, reproducing the synoptic signal as well as short time scale (e.g., diurnal) oscillations. The differences among the three sets of experiments are almost negligible. High and low peaks are correctly predicted and the only relevant discrepancy is found at AA where an underestimation of about 2 hPa occurs around 5 and 12 February. At S1, the same error affects the forecast, although with a much smaller amplitude. The statistical analysis (not shown) confirms the good performance of the model, with correlation ranging between 0.9 and 0.95.

Comparison between RH measurements and forecast is shown only for two locations, which are however representative of all the other sites. Fig. 8 reveals a general and systematic overestimation of the near-surface humidity of the model, which is more relevant on the eastern side of the Adriatic, and affects similarly all the model experiments. At AA, the general

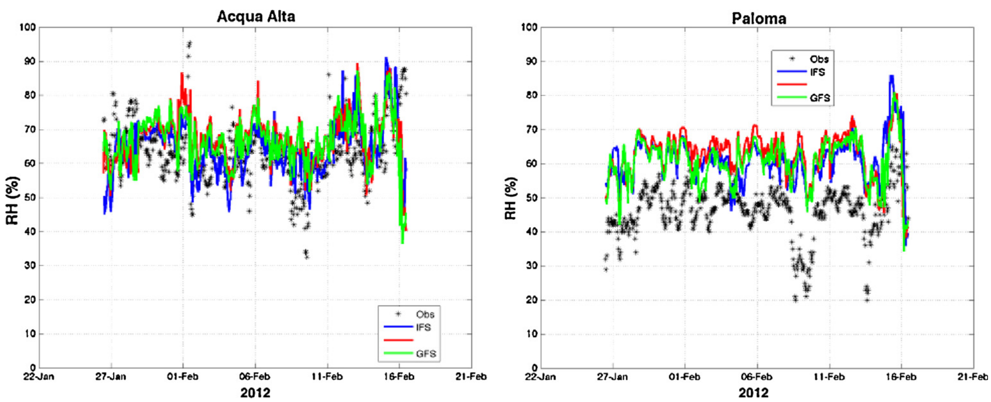

Fig. 8. Time series plot of hourly relative humidity (%) at 2-m above the surface at the station Acqua Alta (AA, left panel) and Paloma (PA, right panel). Black stars indicate measurements, colored lines indicate the results of different MOLOCH experiments: IFS-M (blue), GFS-M (red) and SGFS-M (green). (For interpretation of the references to color in this figure legend, the reader is referred to the web version of this article.)

evolution is correctly forecast, although RH values are predicted about 10% larger than observations. In the Gulf of Trieste, the error is even larger, with differences up to 20% at MB and PA (in VD the error is slightly smaller). Moreover, the model misses the two sudden RH drops on 09 and 14 February. The statistical analysis reveals that the short-time scale oscillations are hardly reproduced by the model, being the correlation below 0.5. Since this error occurs over the sea and in strong wind

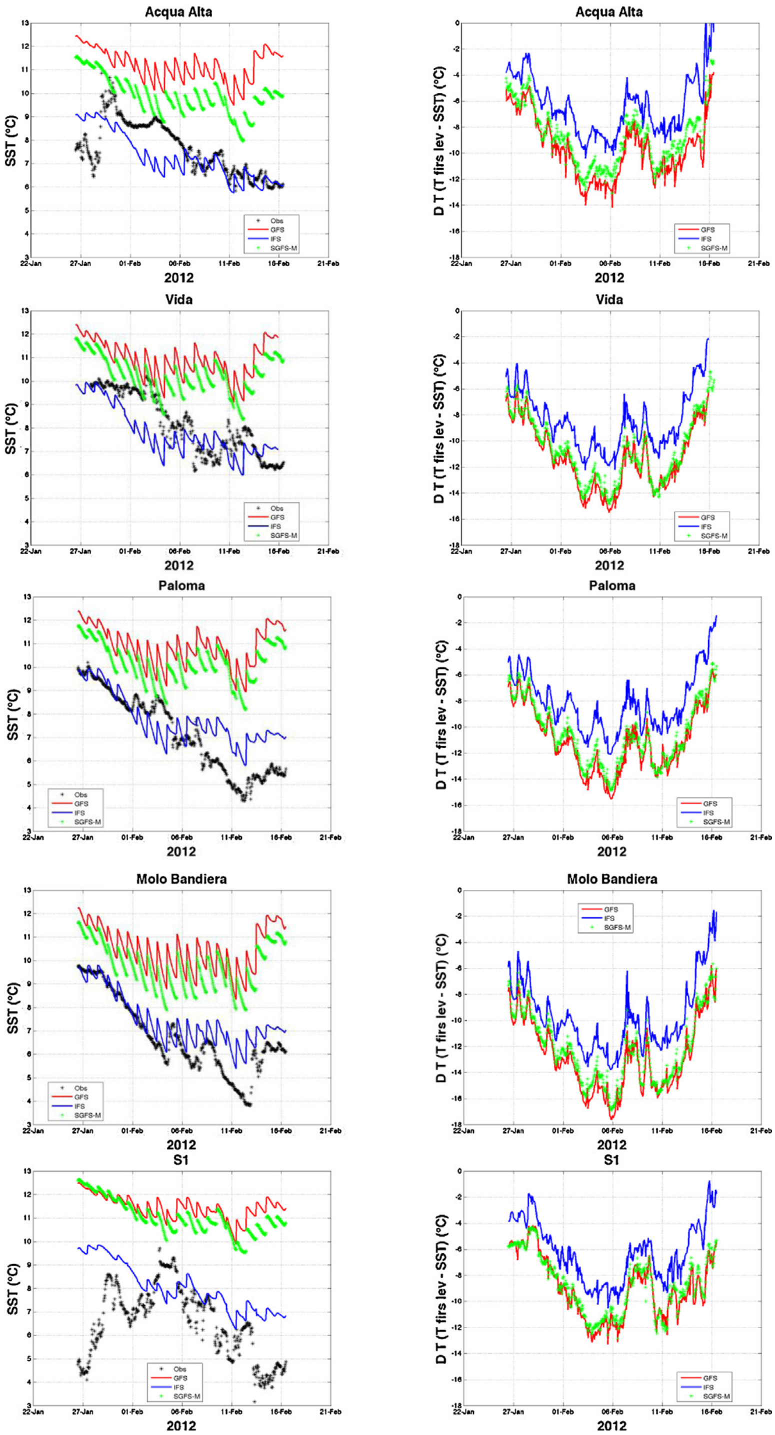

Fig. 9. Time series plot of hourly SST (°C) (left column) and difference between SST and air temperature (°C) at the first model level (approximately 70 m above the ground) at the station Acqua Alta (AA), Vida (VD), Paloma (PA), Molo Bandiera (MB) and S1 buoy. Black stars indicate measurements, colored lines indicate the results of different MOLOCH experiments: IFS-M (blue), GFS-M (red) and SGFS-M (green). (For interpretation of the references to color in this figure legend, the reader is referred to the web version of this article.)

conditions, it can be probably ascribed to the model physical scheme describing the evaporation over ocean. In the present formulation, the skin humidity is considered equal to the saturation value at SST. This means that evaporation rate over sea is infinite and this can be responsible for high value of RH near the surface. This aspect of the model physics needs to be improved; some tests where the skin humidity is reduced depending on the strength of the turbulent mixing (which may be relevant in strong wind conditions) are already under way.

4.3. Comparison of SST and surface fluxes

Hourly time series of SST are shown in Fig. 9. Observations indicate some relevant differences among the analyzed locations at the end of January, before Bora onset. At AA, SST sharply increases between 29 and 30 January, while at VD a constant value around 10 °C is recorded. Differently, in the Gulf of Trieste, MB and PA display a more continuous cooling. Later, SST remains more or less constant at AA during the first days of intense wind before a progressive cooling initiated from 03 February. This latter feature can be identified also at all the other locations, although with some differences in the short time scale fluctuations, as also described in Raicich et al. (2013)Raicich et al. (2013). At S1 the SST evolution is somehow different. The SST rises from 4 °C measured at the beginning of the event up to almost 9 °C recorded on 05 February. Later the SST evolution becomes similar to the other sites, characterized by a constant cooling. The low SST values of the initial period measured at S1 may be ascribable to the direct influence of cold Po river fresh water, as confirmed by low salinity values (29

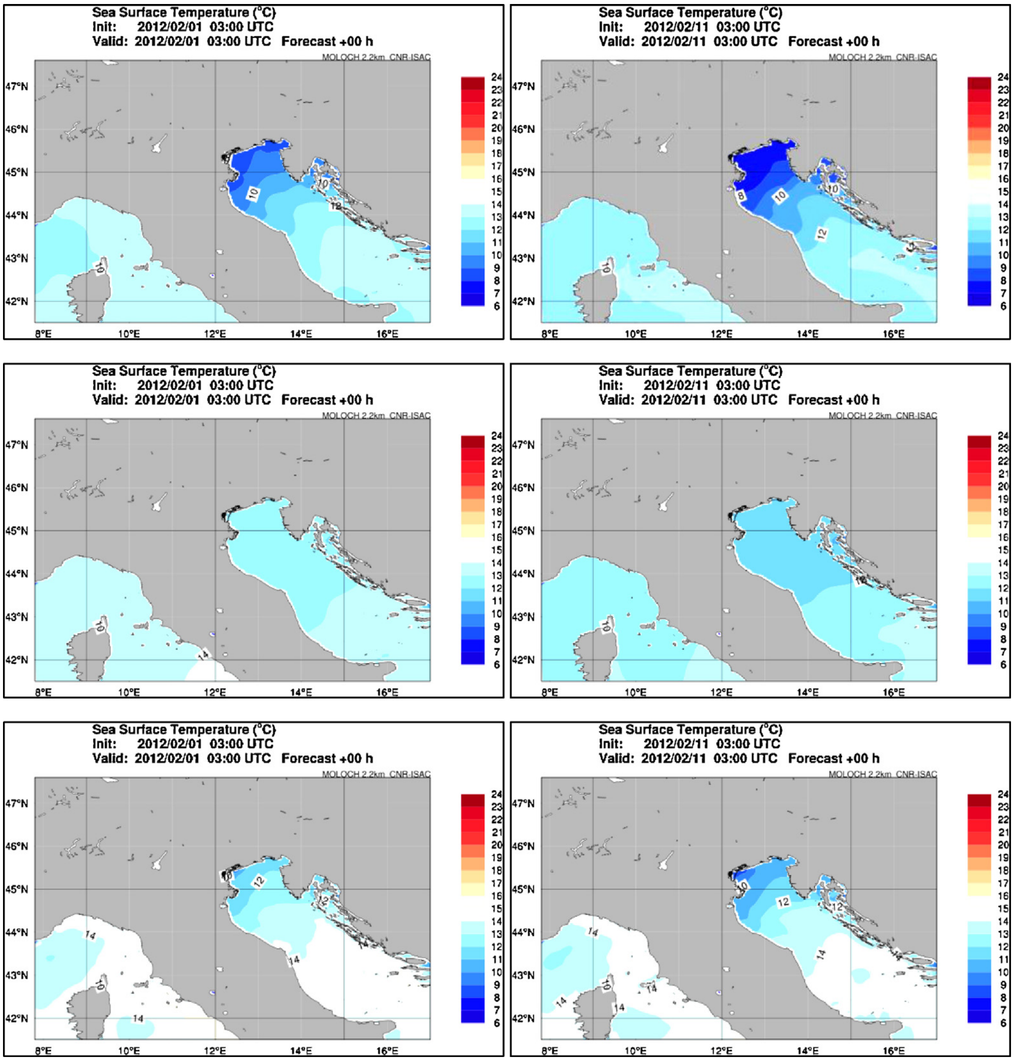

Fig. 10. SST fields interpolated on the MOLOCH grid at the initial time of forecasts: 2 February 2012 (left column) and 11 February 2012 (right column), corresponding with two intense bora episodes. SST data are provided by IFS-ECMWF analysis (top), GFS-NCEP analysis (middle) and MyOcean satellite analysis (bottom).

PSU). The increasing salinity during the second period (37 PSU) indicates a strong nearshore confinement of the Po river plume due to the intense Bora winds.

The comparison with model results in Fig. 9 clearly highlights large uncertainties in the SST forecasts. It is worth noting that the daily SST oscillations in the forecasts are a consequence of the simulations setup, with a new initialization of the run every day as described in Section 2.1. Although MOLOCH produces a cooling during the simulation, due to intense surface

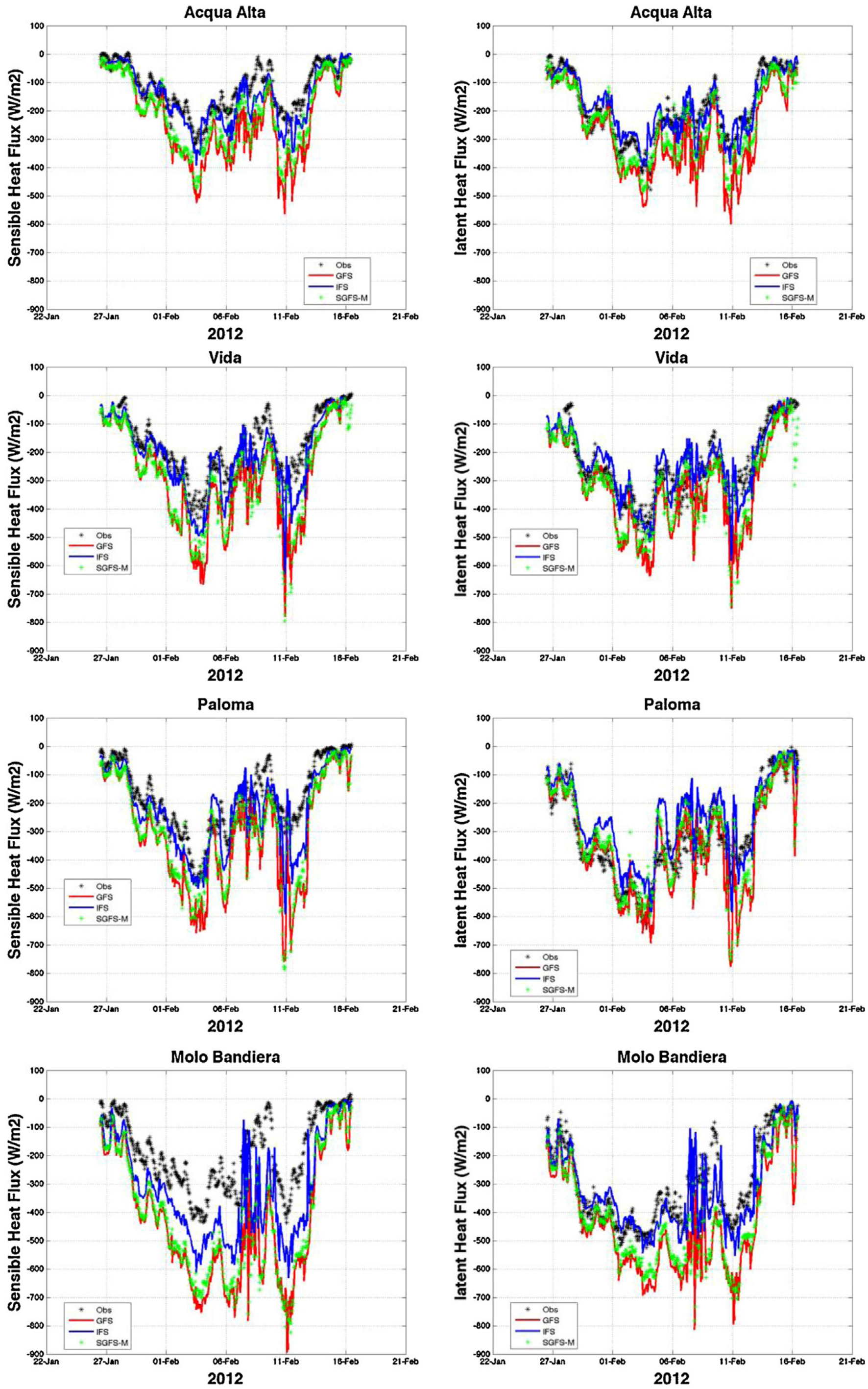

Fig. 11. Time series plot of hourly sensible heat flux (SHF, W/m2) (left column) and latent heat flux (LHF, W/m2) (right column) at different monitoring sites: Acqua Alta (1st row), Vida (2nd row), Paloma (3rd row) and Molo Bandiera (bottom row). Black stars indicate measurements, colored lines indicate the results of different MOLOCH experiments: IFS-M (blue), GFS-M (red) and SGFS-M (green). (For interpretation of the references to color in this figure legend, the reader is referred to the web version of this article.)

fluxes, the SST field imposed in the initial condition from the global model is warmer, thus producing a numerical “jump”. It is evident that, at least along the coastal areas where measurements are available, the accuracy of the SST field provided by the global model is often not satisfactory. This is especially true for the GFS model, whose analyses are affected by a remarkable overestimation of SST, reaching up to 6 °C at the end of the analyzed period, and missing most of the evolution (cooling) observed during the Bora episode. On the other hand, SST field provided by IFS, and the following evolution forecast by MOLOCH, seems to be in much better agreement with the observations, although being affected by some remarkable discrepancies. For example, at AA and VD the model anticipates the cooling, while simulated SST is warmer during the final phase of the event at PA and MB. Moreover, the features characterizing SST evolution at S1 during the first phase of the episode, are not captured properly, since the meteorological model does not take into account the particular circulation of fresh water from the Po river flowing in the Adriatic Sea as described above.

The analysis of SST field at the initial time of MOLOCH forecasts (Fig. 10) for two specific days, 2 and 11 February 2012, clearly shows the differences between the global SST fields employed to initialize the mesoscale models. GFS analysis (and the following MOLOCH simulation, consequently) is not able to capture the rapid space/time variability of the SST field in the northern Adriatic under particular condition like Bora, thus largely overestimating SST values especially along the coastal areas. IFS analysis (and MOLOCH simulation) is more realistic, being characterized by a strong SST meridional gradient, with colder sea water along the northern coast of the Adriatic Sea. SST fields provided by GFS and IFS are the result of two different operational analysis systems (Reynolds and Smith, 1994; Donlon et al., 2012, respectively) that resolve different temporal and spatial scales and use different sets of satellite and/or in situ data. Their quality clearly impact mesoscale model forecasts.

The use of a satellite-derived SST field as initial condition (Fig. 10) improves only slightly the model performance (green line in Fig. 9). As shown in Fig. 10, satellite analysis produces a colder SST than GFS analysis, but still affected by relevant overestimation at least close to the coastal areas. This is probably due to the persistent cloud cover during the considered period, which did not allow to collect new satellite IR observations of the surface temperature to update the optimal interpolation analysis.

Surface heat fluxes over the sea are modulated by wind intensity and strongly depend on the sea-minus-air temperature differences (Dorman et al., 2007). In the PBL parameterization scheme implemented in MOLOCH, the surface fluxes are computed using SST and the temperature at the lowest model level. A comparison (not shown) of this latter variable displays a general close agreement among the different forecasts, with only minor local differences always smaller than 1 °C. Consequently, the different evolution of temperature difference (Fig. 9) between the sea surface and the atmosphere stems from the SST characteristics previously discussed.

The time series of hourly LHF and SHF are shown in Fig. 11. Due to persistent and strong Bora wind and to low air temperatures associated with the cold outbreak (described in Section 3), heat fluxes attain remarkably high values, with maximum observed total heat fluxes up to 800 W/m^2 in correspondence to the coldest period of the event and strong wind intensity. The accuracy of SHF forecasts (Fig. 11) reflects that of air–sea temperature difference (Fig. 9). This is not surprising since, as discussed in the previous Section, forecast wind field is quite accurate and similar among the experiments. Thus, MOLOCH run driven by GFS global model is affected by a remarkable overestimation of surface fluxes, sometimes by a factor of two (indeed the maximum total heat flux at MB reaches 1600 W/m^2). This error is only partially recovered when satellite data are used to define MOLOCH SST initial condition, while simulations driven by IFS are much closer to observations, although still affected by an overestimation during the peak phases. In this case, the overestimation of the fluxes simulated at MB is related to the overestimation of wind speed discussed above, since SST in in very good agreement with observations.

Concerning LHF, as discussed also in Section 4.2, some overestimation may derive from the excess of skin humidity over sea. Moreover, the error affecting SST fields also impacts on the LHF, whose intensity is modulated by the wind speed, stability, and by the air–sea humidity difference (skin minus first model level specific humidity). As described in Section 4.2,

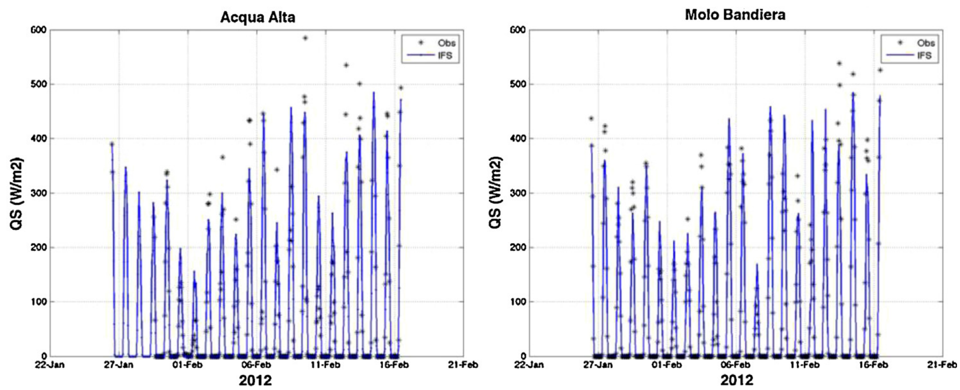

Fig. 12. Time series plot of hourly solar radiation (W/m2) at Acqua Alta (left) and Molo Bandiera (right). Black stars indicate measurements, blue lines indicate the results of IFS-M MOLOCH experiments.

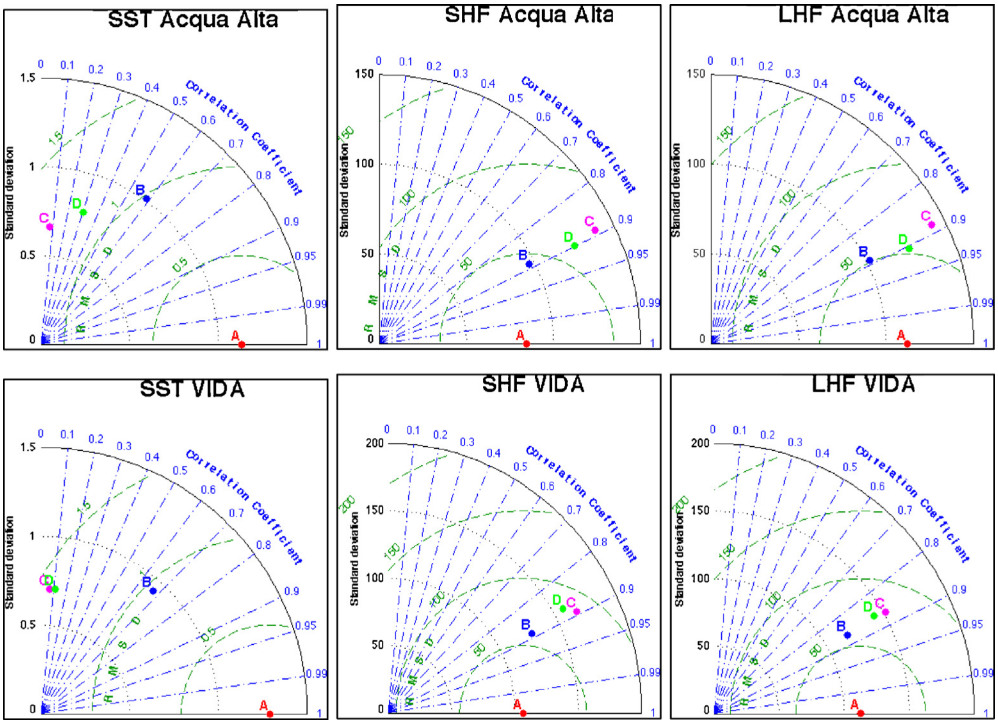

Fig. 13. Taylor diagram for SST (left column), sensible heat flux (center column) and latent heat flux (right column), at Acqua Alta (top) and Vida (bottom). Colored dots indicate observations (red) and MOLOCH experiments results: IFS-M (blue), GFS-M (purple), SGFS-M (green). (For interpretation of the references to color in this figure legend, the reader is referred to the web version of this article.)

at the sea surface the skin humidity is specified as the value at saturation. Therefore, it strongly depends on SST: if SST is overestimated, it is reasonable to expect LHF larger than observed, given a good forecast of the wind field. Consistently, Fig. 11 shows that an overestimation of LHF affects the forecasts driven by GFS global model, while a better agreement between model and observations is attained for the forecasts initialized with IFS analyses. The error becomes larger during intense wind periods, when the value of observed fluxes exceeds 300 W/m^2.

Finally, forecasts of incoming solar radiation have been compared to observations available at several location in the northern Adriatic, in order to validate also this contribution to the radiative balance at the surface. Fig. 12 displays the results at AA and MB (similar results for PA are not shown). Since the differences among the experiments are not relevant, for sake of clarity only the results concerning MOLOCH simulation driven by IFS are presented. Observed values of solar radiation reaching up to 500 W/m^2 are attained in absence of cloud cover. The agreement between forecasts and observations is satisfactory and the differences in radiation peaks, occurring only in specific days of the period, generally do not exceed 50 W/m^2. These differences are certainly ascribable to error in local cloud cover forecasts.

Statistical analysis (Table 2) and Taylor diagram (Fig. 13, only for AA and VD that are considered representative of all the other stations) indicate that all the MOLOCH simulations are able to correctly reproduce the temporal evolution of heat fluxes, since correlation values are quite high. However, the overestimation of fluxes and in particular the different error associated with SST in the three sets of simulations is also highlighted. Mihanović et al. (2013) have also found some differences between observed fluxes at AA and one-way coupled model simulation results: although correctly reproducing the temporal evolution of heat fluxes, the coupled system COSMO-ROMS overestimated the fluxes by about 10% on average, but with errors exceeding 200 W/m^2 on specific instant during the period. The overall model performance presented is comparable with that of MOLOCH driven by IFS data (Miglietta et al., 2013).

The Taylor diagrams for SST (Fig. 13) underline the differences among the MOLOCH runs driven by GFS (GFS-M), IFS (IFS-M) and initialized with satellite SST field (SGFS-M). For example at AA, GFS-M presents a very low correlation factor of 0.1, which improves in SGFS-M rising up to 0.3, but still far from IFS-M correlation factor of 0.6. The mean SST values (Table 2) show that GFS-M and SGFS-M overestimate the SST of 3.5 °C in general for all stations.

5. Conclusion

The Adriatic Sea is regularly affected by cold and strong northeasterly Bora winds, especially during the winter season. Bora events are characterized by intense surface heat and moisture loss and are dominated by air–sea exchange dynamics. Turbulent surface (latent and sensible) heat fluxes and sea surface temperature (SST) are two important parameters that characterize intense air–sea interactions typical of Bora events, and their accurate simulation is required in order to properly describe and understand atmospheric and ocean circulation processes (Boldrin et al., 2009).

This study focused on the longest Bora episode (25 January–15 February 2012) in the northern Adriatic in the last 35 years (Benetazzo et al., 2014), characterized by exceptionally persistent winds that caused significant effects for both atmospheric and oceanic circulation. A number of short-range high-resolution atmospheric simulations have been performed using BOLAM–MOLOCH models, covering the entire period. In particular, two sets of simulations, driven by different global model dataset providing initial and boundary conditions (GFS-NCEP, IFS-ECMWF), have been performed. An additional set of experiments, using the same global model (GFS-NCEP) but a different SST field (from satellite analysis) as initial condition, has also been performed in order to investigate in more detail the impact of SST definition on the MOLOCH simulation results. Models performance has been evaluated in terms of variables of interest for oceanographic application, such as near-surface temperature, wind and relative humidity, surface pressure, surface heat fluxes and solar radiation, and SST. Validation has been undertaken trough a comparison with available surface data (buoys and platforms), while SAR retrievals have been used to evaluate model wind fields on a larger scale.

The comparison shows that the different sets of MOLOCH forecasts provide very similar results in terms of wind speed and direction, in close agreement with the observations, in spite of a slight tendency to overestimate the wind peaks. Wind forecasts are less accurate in correspondence of the S1 buoys, which is not continuously affected by Bora and presents a much more variable wind evolution. In this specific site, MOLOCH reveals some difficulties in simulating the observed wind direction, which is often characterized by deflection along the Italian coast, as also shown by Alpers et al. (2009). The comparison with the ASAR retrieved sea surface wind confirms the ability of the model in reproducing realistically the wind field over the northern Adriatic basin in correspondence with a period of very intense Bora, characterized by localized and intense low-level wind jets and wake areas in between. Also the surface pressure as well as the air temperature evolution is well captured by the model, the latter showing only a slight overestimation during the Bora coldest and strongest phases, while a systematic overestimation of 2-m relative humidity turns out to affect all the experiments at the monitoring stations located over the sea.

The most important uncertainties are in the SST forecasts and consequently in the prediction of latent and sensible heat fluxes. This is especially true for the simulations driven by GFS global model, whose analyses are affected by a remarkable overestimation of SST (up to 6 °C), at least in the analyzed locations close to the coast, and miss most of the evolution (cooling) observed during the Bora episode. Since the surface fluxes in the model PBL scheme are modulated by the wind speed and by the difference between the SST and the lower model level temperature, errors in the SST result in a remarkable overestimation of the fluxes, up to a factor of two, in the GFS-driven simulations. These errors are only partially recovered when satellite data are used to define MOLOCH SST initial condition. However, the impact of satellite analyses was probably limited by the persistent cloud cover, which prevented the ingestion of fresh IR observations to update the Optimal Interpolation procedure. On the other hand, SST field provided by IFS allows a much better forecast of surface heat fluxes, in better agreement with the observations, although some remarkable discrepancies remains, which are anyway comparable with SHF and LHF difference found at AA by Mihanović et al. (2013). The global operational analysis method employed (Donlon et al., 2012) for the IFS is based on the OSTIA system, which uses satellite data also in the Microwave channels and in-situ observations, and it is therefore capable to determine the SST field even in cloudy conditions, at variance with the method applied for the GFS analysis (Reynolds and Smith, 1994), which relies exclusively on IR satellite measurements.

In order to provide a quantitative assessment of the results, Taylor Diagrams have been computed for several variables. The good agreement between simulation results and observations of wind, pressure and temperature is indicated by high value of correlation (0.8-0.9), low root mean square difference values and standard deviation close to observations. Moreover the Taylor diagrams confirm the small differences among the different simulations. The statistical analysis indicates that MOLOCH simulations are able to reproduce the correct temporal evolution of heat fluxes, which is mainly modulated by the wind speed, since correlation values are quite high (0.85). However, a large overestimation is highlighted for simulation driven by GFS model. The present analysis clearly points out that large overestimation of SST in GFS analysis in the narrow northern Adriatic basin is the main reason for the discrepancies between in situ and model forecast latent and sensible heat fluxes. Satellite SST can only partially recover this error, especially in case of persistent cloud cover.

Although the particular and limited period of analysis does not allows for robust conclusions, this study seems to indicate that the best option for SST initialization, when dealing with operational forecasts, is represented by ECMWF analyses. However, they are not widely available in real time, so that alternatives may be required. For different applications such as validation, satellite estimates re-elaborated without real time constraints, may represent a suitable product, given also the high horizontal resolution.

This study can be considered as a first step toward a more detailed investigation of the exceptional Bora episode, which provides very useful information for further analyses and model developments. In particular, the current slab ocean model allows for a too fast cooling during these extreme conditions, thus suggesting the necessity to use a deeper sea surface layer (larger heat capacity) in the presence of strong winds which enhance the ocean surface mixing, thus the thermocline depth. Also, a revised formulation of the skin humidity over the sea turns out to be necessary when turbulence becomes important, such as during intense wind periods, and impacts on near surface humidity. It is already planned to investigate these aspects also in different atmospheric conditions. It is also planned to evaluate the impact of SST field provided by an ocean circulation model to initialize the NWP forecasts and to assess possible improvements of using a 2-way coupling between ocean and atmospheric models. The impact will be evaluated also in terms of prediction of heavy precipitation occurred in the analyzed period, responsible for exceptional snowfall amount over the Apennines. Even atmospheric simulations at higher horizontal resolution will be performed in order to assess possible improvements in the wind field due to a better described orographic forcing. Preliminary experiments showed that the error in wind direction forecasts observed over the Trieste Gulf is almost recovered when 1-km grid is employed.

Acknowledgements

This work was supported by the Italian flagship project RITMARE. UPO CNR contributed to the maintenance of the CNR observational site.

The authors are grateful to Dr. Fabio Raicich, Dr. Vlado Malačič, Dr. Damir Deželjin, Dr. Boris Petelin for kindly providing in-situ observation data. Thanks also to Dr. Magdalena Balmaseda, Dr. Jonah Roberts-Jones, Dr. Kate Howard, Dr. Bert Katz, Dr. Diane Stokes for providing information concerning different SST analysis methodologies.

References

Alpers, W., Ivanov, A., Horstmann, J., 2009. Observations of Bora events over the Adriatic Sea and Black Sea by spaceborne synthetic aperture radar. Mon. Wea. Rev. 137, 1154–1165.
Artegiani, A., Bregant, D., Paschini, E., Pinardi, N., Raicich, F., Russo, A., 1997. The Adriatic Sea general circulation. Part I: air–sea interactions and water mass structure. J. Phys. Oceanogr. 27, 1492–1514.
Benetazzo, A., Bergamasco, A., Bonaldo, D., Falcieri, F.M., Sclavo, M., Langone, L., Carniel, S., 2014. Response of the Adriatic Sea to an intense cold air outbreak: dense water dynamics and wave-induced transport. Prog. Oceanogr. 128, 115–138. http://dx.doi.org/10.1016/j.pocean.2014.08.015.
Billet, S., Toro, E.F., 1997. On WAF-type schemes for multidimensional hyperbolic conservation laws. J. Comput. Phys. 130, 1–24.
Boldrin, A., Carniel, S., Giani, M., Marini, M., Bernardi Aubry, F., Campanelli, A., Grilli, F., Russo, A., 2009. The effect of Bora wind on physical and bio-chemical properties of stratified waters in the Northern Adriatic. J. Geophys. Res. (Ocean) 114 doi:http://dx.doi.org/10.1029/2008JC004837 C08S92.
Bougeault, P., Lacarrere, P., 1989. Parameterization of orography-induced turbulence in a mesoscale model. Mon. Wea. Rev. 117, 1872–1890.
Buongiorno Nardelli, B., Tronconi, C., Pisano, A., Santoleri, R., 2013. High and ultra-high resolution processing of satellite sea surface temperature data over the Southern European Seas in the framework of MyOcean project. Remote Sens. Environ. 129, 1–16. http://dx.doi.org/10.1016/j.rse.2012.10.012.
Buzzi, A., D'Isidoro, M., Davolio, S., 2003. A case study of an orographic cyclone south of the Alps during the MAP SOP. Q. J. R. Meteorol. Soc. 129, 1795–1818.
Buzzi, A., Davolio, S., Malguzzi, P., Drofa, O., Mastrangelo, D., 2014. Heavy rainfall episodes over Liguria of autumn 2011: numerical forecasting experiments. Nat. Hazard Earth Syst. Sci. 14, 1325–1340.
Carniel, S., Bergamasco, A., Book, J.W., Hobbs, R.W., Sclavo, M., Wood, W.T., 2012. Tracking bottom waters in the Southern Adriatic applying seismic oceanography techniques. Continental Shelf Res. 44, 30–38. doi:http://dx.doi.org/10.1016/j.csr.2011.09.00.
Cesini, D., Morelli, S., Parmiggiani, F., 2004. Analysis of an intense Bora event in the Adriatic area. Nat. Hazards Earth Syst. Sci. 4, 323–337.
Charnock, H., 1955. Wind stress over a water surface. Q. J. R. Meteorol. Soc. 81, 639–640.
Davolio, S., Buzzi, A., Malguzzi, P., 2006. Orographic influence on deep convection: case study and sensitivity experiments. Meteorol. Z. 15, 215–223.
Deardorff, J.W., 1980. Stratocumulus-capped mixed layers derived from a three dimensional model. Boundary Layer Meteorol. 18, 495–527.
Donlon, C.J., Martin, M., Stark, J., Roberts-Jones, J., Fiedler, E., Wimmer, W., 2012. The operational sea surface temperature and sea ice analysis (OSTIA) system. Remote Sens. Environ. 116, 140–158.
Dorman, C.E., Carniel, S., Cavaleri, L., Sclavo, M., Chiggiato, J., et al., 2007. February 2003 marine atmospheric conditions and the Bora over the northern Adriatic. J. Geophys. Res 112 doi:http://dx.doi.org/10.1029/2005JC003134 C03S03.
Drofa, O.V., Malguzzi, P., 2004. Parameterization of microphysical processes in a non hydrostatic prediction model. Proceedings of the 14th International Conference on Clouds and Precipitation (ICCP), Bologna, 19–23 July, pp. 1297–3000.
Enger, L., Grisogono, B., 1998. The response of Bora-type flow to seasurface temperature. Q. J. R. Meteorol. Soc. 124, 1227–1244.
Fairall, C.W., Bradley, E.F., Hare, J.E., Grachev, A.A., Esson, J.B., 2003. Bulk parameterization of air–sea fluxes: updates and verification for the COARE algorithm. J. Climate 16, 571–591.
Gačić, M., Eusebi Borzelli, G.L., Civitarese, G., Cardin, V., Yari, S., 2010. Can internal processes sustain reversals of the ocean upper circulation? The Ionian Sea example. Geophys. Res. Lett. 37 doi:http://dx.doi.org/10.1029/2010GL043216 L09608.
Grazzini, F., 2013. Cold spell prediction beyond a week: extreme snowfall events in February 2012 in Italy. ECMWF Newsl. 136, 31–35.
Grisogono, B., Belušić, D., 2009. A review of recent advances in understanding the meso- and microscale properties of the severe Bora wind. Tellus A 61, 1–16. doi:http://dx.doi.org/10.1111/j.1600-0870.2008.00369.x.
Hersbach, H., Stoffelen, A., Haan de, S., 2007. An improved C-band scatterometer ocean geophysical model function: CMOD5. J. Geophys. Res. 112 (C3), C03006.
Janeković, I., Mihanović, H., Vilibić, I., Tudor, M., 2014. Extreme cooling and dense water formation estimates in open and coastal regions of the Adriatic Sea during the winter of 2012. J. Geophys. Res. (Oceans) 119, 3200–3218. doi:http://dx.doi.org/10.1002/2014JC009865.
Kain, J.S., 2004. The Kain–Fritsch convective parametrization: an update. J. Appl. Meteorol. 43, 170–181.
Kraljević, L., Grisogono, B., 2006. Sea-surface temperature effects on 3D Bora-like flow. Meteorol. Z. 15, 169–177.
Lehner, S., Horstmann, J., Koch, W., Rosenthal, W., 1998. Mesoscale wind measurements using recalibrated ERS SAR images. J. Geophys. Res. 103, 7847–7856.
Malanotte-Rizzoli, P., Artale, V., Borzelli-Eusebi, G.L., Brenner, S., Crise, A., Gačić, M., Kress, N., Marullo, S., Ribera d'Alcalà, M., Sofianos, S., Tanhua, T., Theocharis, A., Alvarez, M., Ashkenazy, Y., Bergamasco, A., Cardin, V., Carniel, S., Civitarese, G., D'Ortenzio, F., Font, J., Garcia-Ladona, E., Garcia-Lafuente, J. M., Gogou, A., Gregoire, M., Hainbucher, D., Kontoyannis, H., Kovacevic, V., Kraskapoulou, E., Kroskos, G., Incarbona, A., Mazzocchi, M.G., Orlic, M., Ozsoy, E., Pascual, A., Poulain, P.-M., Roether, W., Rubino, A., Schroeder, K., Siokou-Frangou, J., Souvermezoglou, E., Sprovieri, M., Tintoré, J., Triantafyllou, G., 2014. Physical forcing and physical/biochemical variability of the Mediterranean Sea: a review of unresolved issues and directions for future research. Ocean Sci. 10, 281–322.
Malguzzi, P., Grossi, G., Buzzi, A., Ranzi, R., Buizza, R., 2006. The 1966 'century' flood in Italy: a meteorological and hydrological revisitation. J. Geophys. Res. 111, D24106.
Miglietta, M.M., Davolio, S., Carniel, S., Benetazzo, A., Della Valle, A., Russo, A., Sclavo, M., 2013. The winter 2012 cold outbreak over the Northern Adriatic Sea: preliminary comparison among data and high resolution operational atmospheric models. Proceedings of the 13th EMS Annual Meeting and 11th European Conference on Applied Climatology (ECAC), Reading, 9–13 September.
Mihanović, H., Vilibić, I., Carniel, S., Tudor, M., Russo, A., Bergamasco, A., Bubić, N., Ljubešić, Z., Viličić, D., Boldrin, A., Malačič, V., Celio, M., Comici, C., Raicich, F., 2013. Exceptional dense water formation on the Adriatic shelf in the winter of 2012. Ocean Sci. 9, 561–572. doi:http://dx.doi.org/10.5194/os-9-561-2013.
Morcrette, J.-J., Barker, H.W., Cole, J.N.S., Iacono, M.J., Pincus, R., 2008. Impact of a new radiation package, McRad in the ECMWF integrated forecasting system. Mon. Wea. Rev. 136, 4773–4798.
Pullen, J., Doyle, J.D., Signell, R.P., 2006. Two-way air–sea coupling: a study of the Adriatic. Mon. Wea. Rev. 134, 1465–1483.

Pullen, J., Doyle, J.D., Haack, T., Dorman, C.D., Signell, R.P., et al., 2007. Bora event variability and the role of air-sea feedback. J. Geophys. Res. 112, C03S18. doi: http://dx.doi.org/10.1029/2006JC003726.

Raicich, F., Malačič, V., Celio, M., Giaiotti, D., Colucci, R.R., Čermelj, B., Pucillo, A., 2013. Extreme air–sea interactions in the Gulf of Trieste (North Adriatic) during the strong Bora event in winter 2012. J. Geophys. Res. (Oceans) 18, 5238–5250. doi:http://dx.doi.org/10.1002/jgrc.20398.

Reynolds, R.W., Smith, T.M., 1994. Improved global sea surface temperature analyses using optimum interpolation. J. Climate 7, 929–948.

Ritter, B., Geleyn, J.F., 1992. A comprehensive radiation scheme for numerical weather prediction models with potential applications in climate simulations. Mon. Wea. Rev. 120, 303–325.

Robinson, A.R., Leslie, W.G., Theocharis, A., Lascaratos, A., 2003. Mediterranean Sea circulation. In: Steele, J.H., Thorpe, S.A., Turekian, K.K. (Eds.), Encyclopedia of Ocean Sciences. Elsevier, Amsterdam, pp. 1689–1705.

Signell, R.P., Chiggiato, J., Horstmann, J., Doyle, J.D., Pullen, J., Askari, F., 2010. High-resolution mapping of Bora winds in the northern Adriatic Sea using synthetic aperture radar. J. Geophys. Res. 115, C04020. doi:http://dx.doi.org/10.1029/2009JC005524.

Stravisi, F., Crisciani, F., 1986. Estimation of surface heat and buoyancy fluxes in the Gulf of Trieste by means of bulk formulas. Boll. Oceanol. Teor. Appl. 4, 55–61.

Taylor, K.E., 2001. Summarizing multiple aspects of model performance in a single diagram. J. Geophys. Res. 106, 7183–7192.

Vatova, A., 1934. L'anormale regime fisico-chimico dell'Alto Adriatico nel 1929 e le sue ripercussioni sulla fauna [in Italian]. Thalassia 1 (8), 1–49.

Vilibić, I., Orlić, M., 2002. Adriatic water masses: their rates of formation and transport through the Otranto Strait. Deep-Sea Res. I 49, 1321–1340.

Vilibić, I., Supić, N., 2005. Dense water generation on a shelf: the case of the Adriatic Sea. Ocean Dyn. 55, 403–415.

Zampieri, M., 2004. Comparison among first, second and third order CBL model. Proceedings of the 16th Symposium on Boundary Layers and Turbulence, 9–13 August, Portland, ME (USA).

Zampieri, M., Malguzzi, P., Buzzi, A., 2005. Sensitivity of quantitative precipitation forecasts to boundary layer parameterization: a flash flood case study in the Western Mediterranean. Nat. Hazard Earth Syst. Sci. 5, 603–612.